EASR

Engineering and Applied Science Research

https://www.tci-thaijo.org/index.php/easr/index

Published by the Faculty of Engineering, Khon Kaen University, Thailand

Thin-layer drying model of jackfruit using artificial neural network in a far infrared dryer

Pothong Praneetpolkrang*[1)] and Kitti Sathapornprasath[2)]

[1)]Department of Industrial Technology, Faculty of Industrial Technology, Rambhai Barni Rajabhat University, Chanthaburi 22000, Thailand
[2)]Department of Mechanical Engineering, Faculty of Engineering, Srinakharinwirot University, Nakhorn-Nayok 26120, Thailand

Received 16 May 2020
Revised 30 July 2020
Accepted 11 August 2020

Abstract

The purpose of this article was to find the optimal model to illustrate the drying behaviors of jackfruit in a far-infrared (FIR) dryer and to examine the drying characteristics. The drying conditions were operated at drying temperatures of 60, 70 and 80 °C. In the empirical models, the Newton, Page, Modified Page, Midilli et al., Two term exponential, Henderson and Pabis, Logarithmic, and Wang and Singh model, were investigated to find the most suitable model. An artificial neural network model was also studied, with drying temperature and time selected as input variables, and MR values selected as output parameters. The dependability of the model was assessed using the R^2, χ^2, RMSE and r statistical criteria. The results showed that for the empirical model, the Page model offered excellent results, while the optimal ANN structure was identified as 2-12-1 with Tan-sigmoid transfer functions.

Keywords: Artificial neural network, Drying kinetics, Jackfruit, Far infrared radiation

1. Introduction

In several tropical countries, the jackfruit (*Artocarpus heterophyllus* Lam) is recognized as one of the most popular fruits [1]. It can be consumed in ripe seed form as an unripe fruit. In the food industry, ripe jackfruit seeds are used to produce many different types of dessert. The jackfruit provides essential nutrients since it contains high amounts of carbohydrates and sugars and various minerals [1]. However, after harvesting, jackfruit ripens and deteriorates quickly due to its high water content, thus it cannot be kept for a long time [1]. So, appropriate handling of the jackfruit after harvesting is essential to prolong its preservation. The water activity of agro-material affect microorganisms causing deterioration, thus water activity control can be used to prevent quality changes in agro-material. Processing dried jackfruit into a snack is one way to increase the market value. The drying processing is important process to decrease the moisture content of fruit and vegetable crops to extend the storage period of these products [2-5]. Several drying methods can be used to preserve agricultural products, such as the fluidized bed, heat pump, rotary, and vacuum techniques [6]. However, each drying method has different advantages and limitations, with the selection of each method dependent on the type of agriculture product and suitability.

Recently, the infrared radiation (IR) drying technique has been extensively used to reduce the water content of crops [6-8]. The IR technique has many attractive advantages, for example, a reduced drying time, energy saving, and production of high quality dried products compared with other methods [5, 6, 8, 9]. According to its wavelength, there are three levels of infrared radiation, or electromagnetic waves, namely near-infrared, middle-infrared and far-infrared [6, 9]. Infrared radiation is energy in the form of electromagnetic waves, which penetrates a material causing some of the radiation to be absorbed, with the molecules vibrating into heat energy [10]. The moisture is heated and spreads to the surface of the material before evaporating into the atmosphere. During drying, the absorption of dry materials is decreased, with reflections and transmissions increased due to the reduced water content [10]. Several previous studies have applied the IR technique for drying food and other crops, for example, Chinese yam [5], ginseng [9], and peppermint leaves [10]. The drying operations are non-linear and complex thermal phenomenon [2, 11, 12], nevertheless, knowledge of the drying operation under suitable conditions is necessary [12]. In drying food products, mathematical models have been applied to explain the relationship between the moisture content and time across different conditions. Empirical models have been the mostly been used predict the correlation of moisture content with time in agricultural materials [2, 12-15]. The empirical models have several different forms of equation (Page, Newton, Logarithm, and other models), with the appropriate model based on the drying method or the properties of the agricultural material [3, 12]. The easy applications of empirical models have led many researchers to use them to analyze the drying process of fruits and other crops. In general, empirical model correlations, which depend only on experimental results, provide a high degree of accuracy, however under certain conditions; they may not be suitable [11].

The Artificial Neuron Network (ANN) is a popular intelligent modeling technique, which is used across various fields due to it being considered an effective method with high accuracy [16, 17]. It has a structure of processing functions similar to the human brain, which adapts itself to the input response according to the rules of learning. The ANN has very powerful tools for solving non-linear problems and complex systems, and has been successfully applied in different engineering fields [11, 18, 19].

*Corresponding author. Tel.: +088 080 8859
Email address: pothong.p@rbru.ac.th
doi: 10.14456/easr.2021.20

In terms of a drying system, an ANN can be used to control, model, and optimise the process [15]. In addition, the ANN model can be applied to explain the drying behaviors of various agricultural products [11, 16, 17, 20]. However, to date, there has been no model related to drying jackfruit in a far-infrared dryer in the previous reports. Therefore, the purpose of this work was to examine the drying kinetics of jackfruit and develop models for the prediction of its moisture ratio when dried in a far-infrared dryer.

2. Materials and methods

2.1 Samples and drying experimentation

In this work, the sample materials were ripe jackfruit (Figure 1), purchased from a market in Pathum Thani, Thailand. The ripe jackfruit bulb was cut into pieces, approximately 1 cm wide, 5 cm long and 0.5 cm thick. The jackfruit pieces were packed into a plastic bag and stored in a refrigerator (4 ^{o}C) to protect against water evaporation. Before commencing the drying experiment, the samples were spread out to obtain a thermal equilibrium with the room temperature. The drying experiments were operated at three drying temperatures; 60, 70 and 80 °C. In order to achieve the desired temperature, the far-infrared dryer was started at least 1 hr before commencement of the drying test. The thin layers of jackfruit piece samples (approximately 500 g) were subsequently spread on a tray for testing. The sample weight was recorded every 30 minutes throughout the experiment until the weights were constant. Each drying experiment was reproduced three times in each condition. Upon the sample weight not changing, the drying system was stopped.

Figure 1 The jackfruit samples

2.2 FIR dryer set-up

In this study, the far-infrared (FIR) dryer was a laboratory scale (Figure 2), which had a drying chamber (stainless steel) with dimensions of 45×45×40 cm^3 (L×W×H). The FIR lamp had a power of 500 W and was located at the top of the chamber. A stainless steel sample tray, with dimensions of 20×30cm^3, was placed below the FIR lamp at a distance of approximately 15 cm. A digital balance was located under the tray for measuring the weight of the samples and was connected to a recording apparatus to note the sample weight data. The temperature inside the chamber was measured by a thermocouple (type k) and controlled by a PID controller (SHINKO, JCS-33A, Japan). The total electric energy consumed (FIR lamps and electric fan) of the drying system was measured using the Watt-hour meter. The glass wool insulation, with a 5 cm thickness, was covered inside the wall of the drying chamber to prevent heat loss.

The drying kinetics of jackfruit was determined in terms of the moisture ratio (MR) and drying rate (DR). The moisture ratio (MR) reflected the remaining moisture of the jackfruit, as defined by equation (1) [2, 21]:

$$\text{Moisture Ratio (MR)} = \frac{M_t - M_{eq}}{M_{in} - M_{eq}} \quad (1)$$

The drying rate was defined using equation (2) [2, 21]:

$$\text{Drying rate (DR)} = \frac{M_{t+dt} - M_t}{dt} \quad (2)$$

where M_t, M_{in}, M_{eq} and M_{t+dt} is the remaining moisture content (MC) at any drying time, the initial moisture content, the equilibrium moisture content, and the moisture content at t_{+dt}, respectively. For a long time drying, the M_{eq} value in equation (1) is eliminated since it is very small [2].

2.3 The specific energy consumption (SEC)

The energy used in the drying system is considered a factor in determining the efficiency of the far-infrared dryer. The SEC value is used as an indicator of the energy efficiency of a drying system. The SEC value shows the energy used to vaporize the water from the product. The SEC value computed using the equation (3) [8, 13]:

$$SEC = \frac{E_{total}}{m_{water}} \quad (3)$$

where E_{total} is the total energy consumption (kW.h), and m_{water} is the mass of moisture removed from the samples (kg).

2.4 The evaluation of the moisture diffusivity

The moisture diffusion coefficient is a parameter for indicating the water movement within a material; it can be obtained from the diffusion equation according to Fick's law. Knowledge of effective moisture diffusivity (D_{eff}) is important to understanding the mass transport in agricultural materials. For the D_{eff} value of jackfruit, it was considered that the jackfruit pieces assumed an infinite slab, with the D_{eff} computed using equation (4) [7, 8]:

$$MR = \frac{8}{\pi^2}\sum_{n=0}^{\infty}\frac{1}{(2n+1)^2}\exp\left(\frac{-(2n+1)^2 D_{eff}\pi^2 t}{4L^2}\right) \quad (4)$$

In order to analyze the data, D_{eff} values were calculated using nonlinear regression of the experimental moisture content and drying time. The jackfruit drying process takes a relatively long time, thus resulting in the last term of equation (4) to be very small. Hence, we can only analyze the first term using equation (5) [7, 8]:

$$Ln(MR) = Ln\frac{8}{\pi^2} - \frac{D_{eff}\pi^2 t}{4L^2} \quad (5)$$

where L is the half-thickness of the slab, m

For calculating D_{eff} values, the straight line with a slope (K) was achieved from plotting ln (MR) with time, as follows [7, 8]:

$$k = \frac{D_{eff}\pi^2 t}{L^2} \quad (6)$$

2.5 The water activity energy

During the drying process, water activity energy is associated with drying temperature variables since it has an influence on the drying rate. The relationship between the D_{eff} value and the drying temperature is described using Arrhenius's equation [7, 22]:

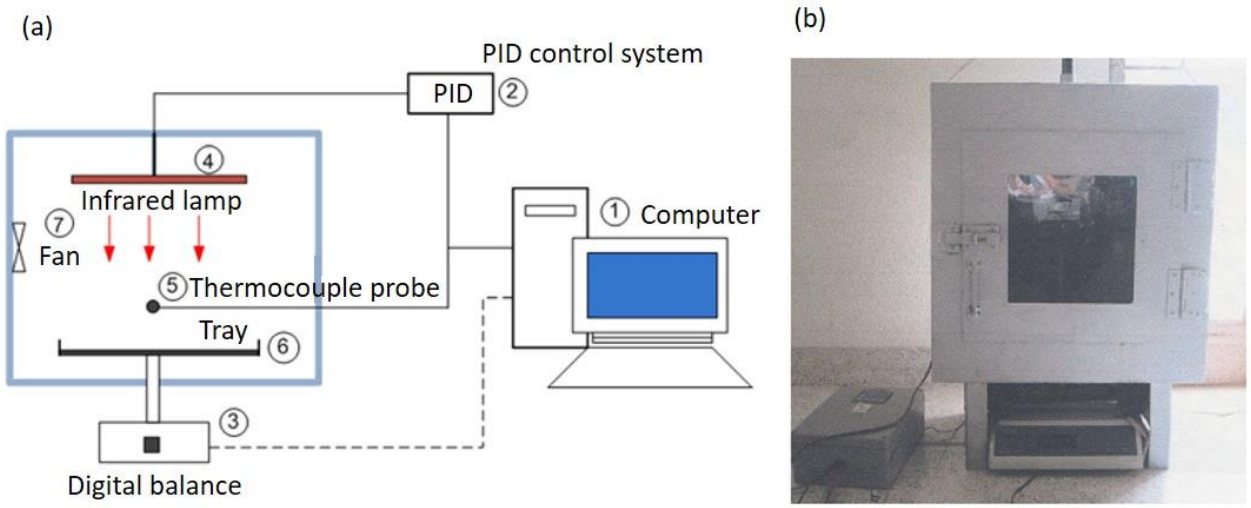

Figure 2 The schematic diagram of the FIR dryer (a) layout (b) lab scale prototype

Table 1 Mathematical models

Model no.	Model name	Model	Reference
1	Newton	MR=exp(-kt)	[2]
2	Page	MR=exp(-kt^n)	[3]
3	Modified Page	MR = xp(-(kt)^n)	[4]
4	Midilli et al.	MR =aexp(-kt^n)+bt	[10]
5	Two term exponential	MR=aexp(-kt)+ (1-a)exp(-kat)	[23]
6	Henderson and Pabis	MR=aexp(-kt)	[24]
7	Logarithmic	MR = aexp(-kt)+c	[25]
8	Wang and Singh	MR=a*t^2+b*t+1	[26]

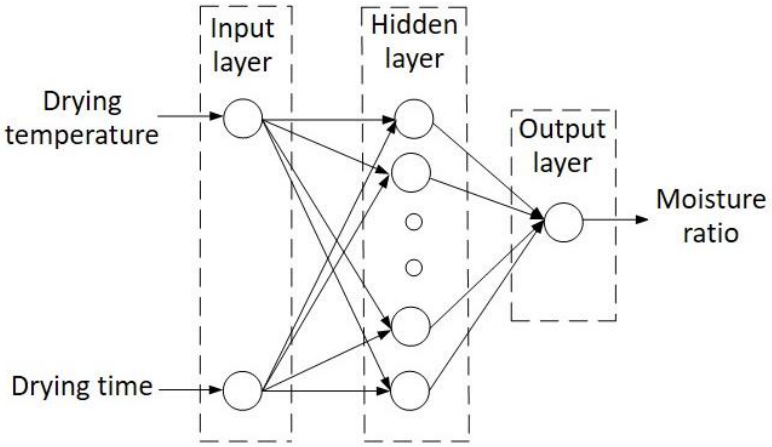

Figure 3 The neural network architecture used in this work

$$D_{eff} = D_o\left(-\frac{E_a}{RT}\right) \quad (7)$$

where D_0, E_a, R and T are the constants in the Arrhenius equation (m^2/s), the activation energy is measured in (kJ/mol), the universal gas constant in (kJ/mol K) and the drying air temperature in (K).

2.6 The empirical model

In order to identify an optimal model to explain the drying behaviour of jackfruit, eight models were assessed (Table 1). The Matlab software package (Matlab R2019a) was used to analyse the drying parameters using nonlinear regression of moisture content over time.

2.7 Neural network model development

Artificial neural network (ANN) is a branch of artificial intelligence, which is created by simulating the processing characteristics of the human brain with mathematical models. Many types of neural network structures include single-layer perceptron, multilayer perceptron and recurrent network applied for modeling in various disciplines [11, 15]. The multilayer perceptron ANN models are popularly used for modeling in drying process operations due to its strong capacity for process modeling and prediction [11, 14, 27]. The multilayer perceptron ANN model used in this work is showed in Figure 3. The structure of the network consisted of two input variables (drying temperature and drying time), while the MR value was used as the output variable. The description of the input and output variables are shown in Table 2. To obtain the optimum network structure, Three types of transfer function in hidden layers were used: Tan - sigmoid, Log - sigmoid, and Pure - Linear, with 20

Table 2 Description of input and output parameters for the ANN models

Types	Parameters	Units	Range
Input	Drying temperature	°C	60-80
	Drying time	min	0-720
Output	Moisture ratio	-	0-1

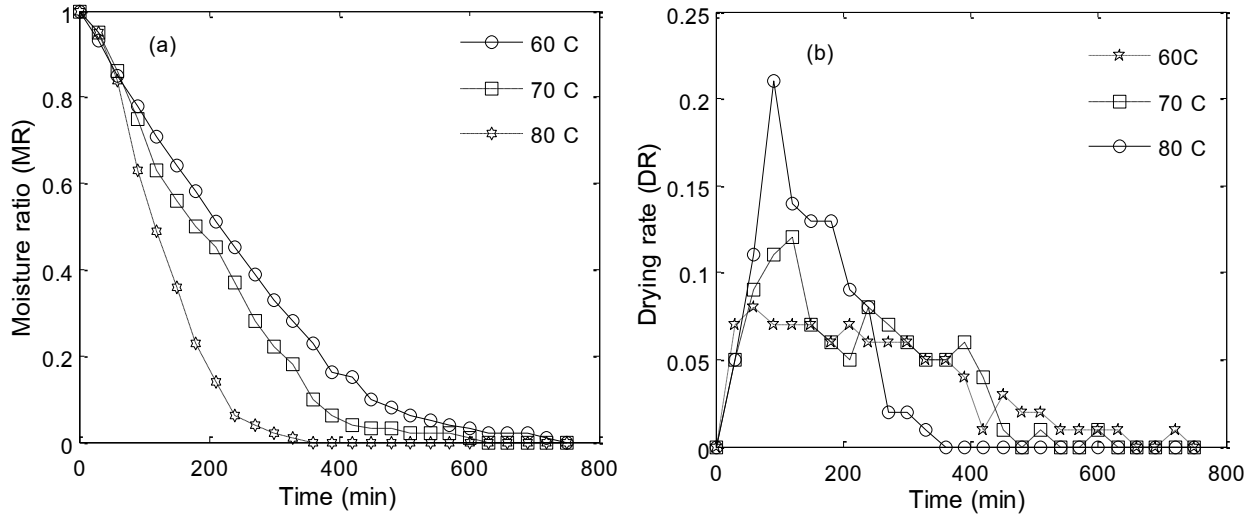

Figure 4 The plot of (a) drying curve, (b) drying rate at temperatures between 60-80 °C

numbers of neurons (range from 1 to 20), were tested to find the optimum model, with the linear activation function applied for the output layer. The Levenberg-Marquardt (trainlm) algorithm was used for training the network. The total drying data were divided randomly into three parts: training (70%), validation (15%), and the remainder used for testing (15%). The development of the ANN model was created using the MATLAB software package.

2.8. Model performance evaluation

In this work, the coefficient of determination (R^2), reduced chi square (χ^2), root mean square error (RMSE) and the coefficient of correlation (r) statistical methods were used as parameters to indicate accuracy of the model prediction. According to nonlinear regression, the drying constants and the statistical results of the models were estimated using the Matlab software package. The statistical indices were computed using the following equations [2, 10, 21, 27]:

$$R^2 = 1 - \left[\frac{\sum_{i=1}^{N}\left(MR_{pre} - MR_{ob}\right)^2}{\sum_{i=1}^{N}\left(\overline{MR_{pre}} - MR_{ob}\right)^2}\right] \quad (8)$$

$$\chi^2 = \frac{\sum_{i=1}^{N}\left(MR_{ob} - MR_{pre}\right)^2}{N - n} \quad (9)$$

$$RMSE = \left[\frac{1}{N}\sum_{i=1}^{N}\left(MR_{ob} - MR_{pre}\right)^2\right]^{1/2} \quad (10)$$

where MR_{ob}, MR_{pre} and $\overline{MR_{pre}}$ are the observed MR value, the predicted MR value, and the average MR predicted value, respectively.

3. Results and discussion

3.1 The drying behaviour of jackfruit

The drying behaviours of jackfruit in a far-infrared dryer at temperatures between 60-80 °C are presented in Figure 4. The moisture ratio (MR) curves plotted against drying time are displayed in Figure 4(a). The influence of drying temperature can be observed to considerably affect MR values. At a high drying temperature, the moisture content of the jackfruit decreased at a faster rate compared with lower temperatures; likely due to the increased rate of heat transfer and water evaporation rate, resulting in a reduced drying time [4, 7, 9, 10, 22-24]. At the drying temperatures of 60, 70 and 80 °C, the final moisture content was achieved at a drying time of 720, 610 and 380 min respectively. Increasing the drying temperature from 60 °C to 70 °C reduced the drying time by 15.3%, while increasing the drying temperature from 60 °C to 80 °C reduced the drying time by 47.2%. Figure 4(b) displays the change in drying rate overtime at temperatures between 60-80 °C. The drying rates can be observed to be relatively high at the beginning of the drying process, before rapidly decreasing over time. A higher drying temperature caused an increased drying rate, with the highest values attained at a drying temperature of 80 °C. Our experimental results are in line with previous findings [2, 4, 7, 9, 10, 21-24].

3.2 The calculation of specific energy consumption

The specific energy consumption (SEC) of drying jackfruit in the far-infrared dryer at 60, 70, and 80 °C is displayed in Figure 5. The results demonstrate that the SEC values decreased with an increased drying temperature. The higher drying temperatures led to an increase in the drying rate and a reduction in the drying time of the jackfruit. As a result, the energy used was also observed to decrease. The highest SEC (6.17 kWh/kg water) occurred data drying temperature of 60 °C, whereas the lowest SEC (5.38 kWh/kg water) was recorded at 80 °C. The SEC values required for drying the jackfruit were 6.17, 5.77 and 5.38 kWh/kg water at 60, 70 and 80 °C, respectively. Our results correspond with previous findings [9].

3.3 The evaluation of the empirical model

The statistical indices and drying constant values were determined using nonlinear regression (Table 3). The highest values of R^2 and r, and the lowest values of χ^2 and RMSE provide an indication of an accurate prediction. The results

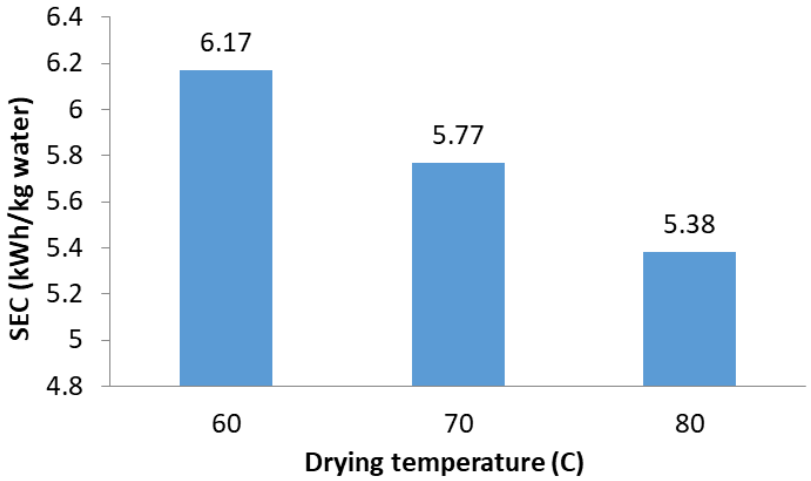

Figure 5 The specific energy consumption (SEC) of drying jackfruit

Table 3 The statistical model indices at different temperatures

Model no.	Temperature (°C)	Model Constants	R^2	χ^2	RMSE	r
1	60	k = 0.003949	0.9600	0.00114	0.0649	0.9924
	70	k = 0.004811	0.9534	0.00805	0.0711	0.9911
	80	k = 0.01233	0.9979	0.00095	0.0143	0.9535
		Average	**0.9704**	**0.0034**	**0.0501**	**0.9790**
2	**60**	**k = 0.0003362, n = 1.431**	**0.9967**	**0.00062**	**0.0189**	**0.999**
	70	**k = 0.0002949, n = 1.504**	**0.9955**	**0.00079**	**0.0224**	**0.9978**
	80	**k = 0.000103, n = 1.846**	**0.9993**	**0.00019**	**0.0088**	**0.9996**
		Average	**0.9972**	**0.00050**	**0.0167**	**0.9988**
3	60	k = -0.8342, n = -0.004725	0.9754	0.00315	0.0431	0.9913
	70	k = 0.6381, n = 0.00752	0.9707	0.00304	0.0476	0.9982
	80	k = 0.1773, n = 0.04199	0.9658	0.00418	0.0596	0.9702
		Average	**0.9706**	**0.00346**	**0.0501**	**0.9866**
4	60	k = 0.0002559, a = 0.9691, b = -2.115×10^{-5}, n = 1.467	0.9954	0.00085	0.01961	0.9982
	70	k = 0.0002588, a = 0.9847, b = -1.186×10^{-5}, n = 1.522	0.9949	0.00098	0.02584	0.9975
	80	k = 0.0001096, a = 1.003, b = 9.178×10^{-7}, n = 1.834	0.9982	0.00039	0.00927	0.9986
		Average	**0.9962**	**0.0007**	**0.0182**	**0.9981**
5	60	k = 5.203, a = 0.0007569	0.9683	0.00358	0.05170	0.9924
	70	k = 6.542, a = 0.0007303	0.9706	0.00287	0.04209	0.9912
	80	k = 15.41, a = 0.0004826	0.968	0.00361	0.05300	0.984
		Average	**0.9690**	**0.0034**	**0.04893**	**0.9892**
6	60	k = 0.004337, a= 1.109	0.9714	0.00414	0.0560	0.9891
	70	k = 0.005828, a = 1.243	0.9756	0.00409	0.0525	0.9841
	80	k = 0.01493, a = 2.058	0.9952	0.00083	0.0224	0.9238
		Average	**0.9807**	**0.0030**	**0.0436**	**0.9657**
7	60	k = 0.003126, a = 1.202, c = -0.1448	0.9893	0.00394	0.0349	0.9955
	70	k = 0.004803, a = 1.232, c = -0.06325	0.9858	0.00543	0.04289	0.9921
	80	k = 0.007667, a = 1.172, c = -0.03376	0.9921	0.00037	0.0294	0.9841
		Average	**0.9891**	**0.0032**	**0.0357**	**0.9906**
8	60	a = 2.02×10^{-6}, b = -0.00284	0.997	0.00067	0.0181	0.9989
	70	a = 2.707 $\times10^{-6}$, b = -0.00333	0.9901	0.00174	0.0334	0.9961
	80	a = 4.023 $\times10^{-6}$, b = -0.00421	0.9033	0.00940	0.1004	0.9606
		Average	**0.9635**	**0.0039**	**0.0506**	**0.9852**

Table 4 The D_{eff} values of jackfruit at temperatures between 60-80 ◦C.

Temperature (◦C)	D_{eff} (m^2/s) x 10^{-7} m^2/s	E_a(kJ/mol)
60	4.94	39.24
70	6.18	
80	10.90	

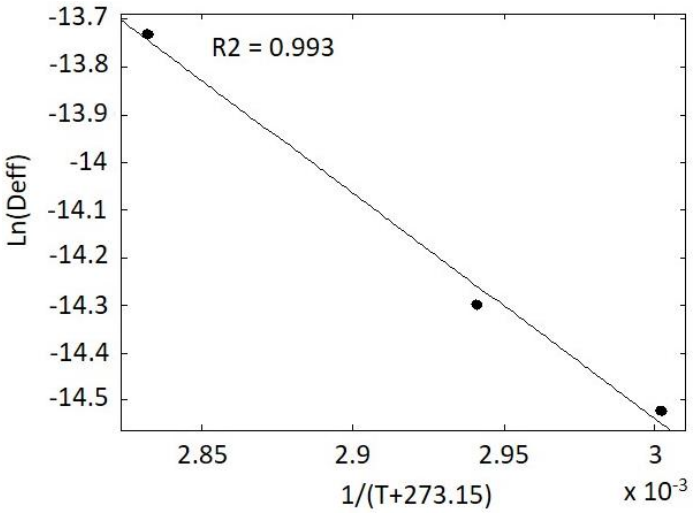

Figure 6 The plot of ln(D_{eff}) vs. 1/(T+273.15) at drying temperature of 60-80 ◦C.

demonstrated that all predicted models fitted the observed drying data with high accuracy (R^2,>0.9033 (range: 0.9033-0.9993); r,>0.9102 (range: 0.9102-0.9996); χ^2,<0.00940 (range: 0.00019-0.00940); RMSE, <0.1004 (range: 0.0088-0.1004). Therefore, all the models can be applied to predict the drying kinetics of jackfruit in a far-infrared dryer. However, out of the 8 model equations, the page model returned the best prediction values across all the drying conditions (range: R^2, 0.9967 to 0.9993; r, 0.9978 to 0.9996; RMSE, 0.0088 to 0.0224; χ^2, 0.00019 to 0.00079). Alternatively, the Wang and Singh model provided the poorest prediction values (range: R^2, 0.9033 to 0.997; r, 0.9606 to 0.9989; RMSE, 0.0181 to 0.1004; χ^2, 0.00940 to 0.00067). Accordingly, our results suggest that the page model was the optimal model for estimating the change of MR when drying jackfruit. The drying temperature was inserted into the page model equation as follows:

Page model; $MR = \exp(-k*t^n)$
$k = 0.001061-0.00001166T$; $R^2=0.912$
$n = 0.1412+0.02075T$; $R^2=0.930$

where T is drying temperature (°C)

3.4 The computation of D_{eff} and E_a values

The D_{eff} values at drying temperature between 60-80 °C, were computed using Eq. (7). The D_{eff} values were observed to range between $4.94x10^{-7}$-$10.90x10^{-7}$ m^2/s (Table 4), with the lowest and highest D_{eff} values found at the drying temperatures of 60 ◦C and 80 °C, respectively. The effective moisture diffusivity values were found to increase at higher drying temperatures (Table 4). Due to increasing the drying temperature caused to increase in vapor pressure and to accelerate the activity of water molecules of samples, consequently leading to increased the moisture diffusivity [10]. The calculated D_{eff} values are within a similar range of olive pomace at 50-80 °C ($0.68 x10^{-7}$-$2.15x10^{-7}$ m/s^2) [3], yacon slices at 5-45 °C ($1.092x10^{-7}$-$7.388x10^{-7}$ m^2/s) [4], chopped coconut ($0.59902x10^{-7}$-$2.6616 x10^{-7}$ m/s^2) [25], Jew's mallow at 50-70 °C ($0.818 x10^{-7}$-$1.13 x10^{-7}$ m/s^2) [26], treated plums at 60-80 °C ($1.197x10^{-7}$-$4.551x10^{-7}$ m/s^2) [28], potato slices at 50-70 °C ($3.17x10^{-7}$-$15.17x10^{-7}$ m/s^2) [29], and pumpkin slices at 30-70 °C ($0.408x10^{-7}$- $2.35x10^{-7}$ m^2/s) [30].

The effective diffusivity coefficient (Table 4) was described using the Arrhenius equation, Eq. (8). The activation energy values (Ea) were appraised using the slope and intercept of the linear plot, the value of ln(D_{eff}) vs. (1/(T + 273.15)); Figure 6. The obtained straight line represents the uniformity of variation of the effective diffusivity with drying temperature. The results indicated that the calculated E_a value of jackfruit was 39.24 kJ/mol between the drying temperatures of 60-80 ◦C. The achieved Ea values are within the range of 15-40 kJ/mol reported by other researchers [4, 29-31].

3.5 The evaluation of ANN model

In this study, three different types of activation functions (Tan-sigmoid, Log-sigmoid and Pure- Linear) and 20 numbers of neurons (ranges from 1 to 20) were developed to find the best ANN model structure. The optimum number of neurons in hidden layers investigated through trial and error method [32]. The performance of every ANN model was based on the static result values of R^2 and RMSE. The training and testing statistical results of every ANN model is presented in Table 5. In regards to the training phase, the R^2 and RMSE values of the ANN models were between 0.90326 to 0.99977 and 0.0069 to 0.1966, respectively. In regards to the testing phase, the R^2 and RMSE values were between 0.90307 to 0.99975 and 0.00486 to 0.14064, respectively. However, the performance of the ANN model with a Tan-sigmoid activation function and 12 neurons in hidden layer performed better compared with the other ANN models. The R^2 and RMSE values of these models were 0.99977 and 0.0069 in the training data set, and 0.99975 and 0.00486 in the testing data set, respectively. Therefore, the ANN model with a Tan-sigmoid activation function and 12 neurons was selected as suitable to predict the MR of jackfruit in a FIR dryer.

Table 5 The performance of the ANN models with three activation functions.

Number of neuron (hidden layer)	Transfer function	Training		Testing	
		R^2	RMSE	R^2	RMSE
1	Tan-sigmoid	0.98340	0.0672	0.99825	0.05328
	Log-sigmoid	0.98079	0.0558	0.9954	0.04482
	Pure- Linear	0.92113	0.1619	0.91393	0.11472
2	Tan-sigmoid	0.99492	0.0266	0.99477	0.01366
	Log-sigmoid	0.98633	0.0419	0.97726	0.04614
	Pure- Linear	0.9153	0.1238	0.93269	0.10707
3	Tan-sigmoid	0.99707	0.0320	0.99862	0.01229
	Log-sigmoid	0.99829	0.0463	0.99511	0.01338
	Pure- Linear	0.91412	0.1272	0.92795	0.11421
4	Tan-sigmoid	0.99876	0.0127	0.99476	0.01590
	Log-sigmoid	0.99939	0.0224	0.99901	0.01920
	Pure- Linear	0.90486	0.1221	0.95712	0.11205
5	Tan-sigmoid	0.99943	0.0083	0.98825	0.02221
	Log-sigmoid	0.99921	0.0095	0.99925	0.00906
	Pure- Linear	0.96593	0.0600	0.93931	0.11284
6	Tan-sigmoid	0.99962	0.0082	0.99814	0.01593
	Log-sigmoid	0.99722	0.0212	0.96686	0.01588
	Pure- Linear	0.89503	0.1520	0.97905	0.10689
7	Tan-sigmoid	0.99941	0.0093	0.99813	0.02615
	Log-sigmoid	0.99949	0.0120	0.99913	0.01910
	Pure- Linear	0.90326	0.1301	0.92501	0.10867
8	Tan-sigmoid	0.99906	0.0138	0.99904	0.01978
	Log-sigmoid	0.99949	0.0119	0.99857	0.02604
	Pure- Linear	0.91855	0.1464	0.96171	0.10224
9	Tan-sigmoid	0.99954	0.0128	0.99863	0.00552
	Log-sigmoid	0.99925	0.0381	0.99766	0.01651
	Pure- Linear	0.92155	0.1966	0.92357	0.14064
10	Tan-sigmoid	0.99841	0.0132	0.99889	0.01648
	Log-sigmoid	0.99900	0.0108	0.99939	0.00612
	Pure- Linear	0.96322	0.0594	0.92327	0.10771
11	Tan-sigmoid	0.99970	0.0294	0.99931	0.01812
	Log-sigmoid	0.99961	0.0125	0.99604	0.01798
	Pure- Linear	0.90924	0.1336	0.91785	0.11722
12	**Tan-sigmoid**	**0.99977**	**0.0069**	**0.99975**	**0.00486**
	Log-sigmoid	0.99933	0.0265	0.99894	0.01978
	Pure- Linear	0.91692	0.1836	0.93341	0.11095
13	Tan-sigmoid	0.99967	0.0109	0.99944	0.01945
	Log-sigmoid	0.98491	0.0377	0.98886	0.06755
	Pure- Linear	0.91246	0.1680	0.94395	0.10915
14	Tan-sigmoid	0.99963	0.0153	0.99707	0.01337
	Log-sigmoid	0.99940	0.0155	0.99616	0.01027
	Pure- Linear	0.92075	0.1351	0.93768	0.11117
15	Tan-sigmoid	0.99976	0.0073	0.99938	0.01314
	Log-sigmoid	0.99912	0.0099	0.99613	0.03652
	Pure- Linear	0.96354	0.0588	0.95730	0.10950
16	Tan-sigmoid	0.99868	0.0155	0.99731	0.02916
	Log-sigmoid	0.99775	0.0137	0.99964	0.02444
	Pure- Linear	0.90991	0.1641	0.90307	0.10433
17	Tan-sigmoid	0.99877	0.0169	0.99901	0.01754
	Log-sigmoid	0.99955	0.0155	0.99862	0.01290
	Pure- Linear	0.91663	0.1732	0.92486	0.10616
18	Tan-sigmoid	0.99857	0.0278	0.99878	0.02554
	Log-sigmoid	0.99788	0.0351	0.99684	0.02529
	Pure- Linear	0.90561	0.1273	0.86743	0.11768
19	Tan-sigmoid	0.99942	0.0285	0.99926	0.01597
	Log-sigmoid	0.99876	0.0142	0.99950	0.02410
	Pure- Linear	0.92745	0.1912	0.94118	0.11092
20	Tan-sigmoid	0.99917	0.0099	0.99662	0.01326
	Log-sigmoid	0.99861	0.0126	0.99906	0.01094
	Pure- Linear	0.96582	0.0620	0.92612	0.10393

3.6 Comparison of the measured and predicted model values

The measured MR values of the Page model were compared to the predicted values (Figure 7(a)-(b)). It can be observed that the calculated model values were similar to the measured values. The achieved values of R^2 and RMSE were 0.9972 and 0.0167 at drying temperatures between 60-80 ◦C, suggesting that this model has a high degree of accuracy to predict MR during the drying of jackfruit. The plot of the ANN model predicted MR values compared to the experimental data at drying temperatures between 60-80 °C, are displayed in Figure 8(a)-(b). It can be observed that the predicted values had a good agreement (R^2, 0.99975; RMSE, 0.00486) with the actual values (Figure 8b). Consequently, the ANN model is an appropriate model to describe the drying characteristics of jackfruit in a FIR dryer.

4. Conclusions

In this work, a suitable model was identified to describe the drying kinetics of jackfruit in a far-infrared (FIR) dryer. The experiments were conducted at drying temperatures of 60, 70 and 80 °C, respectively. The results showed that drying temperature

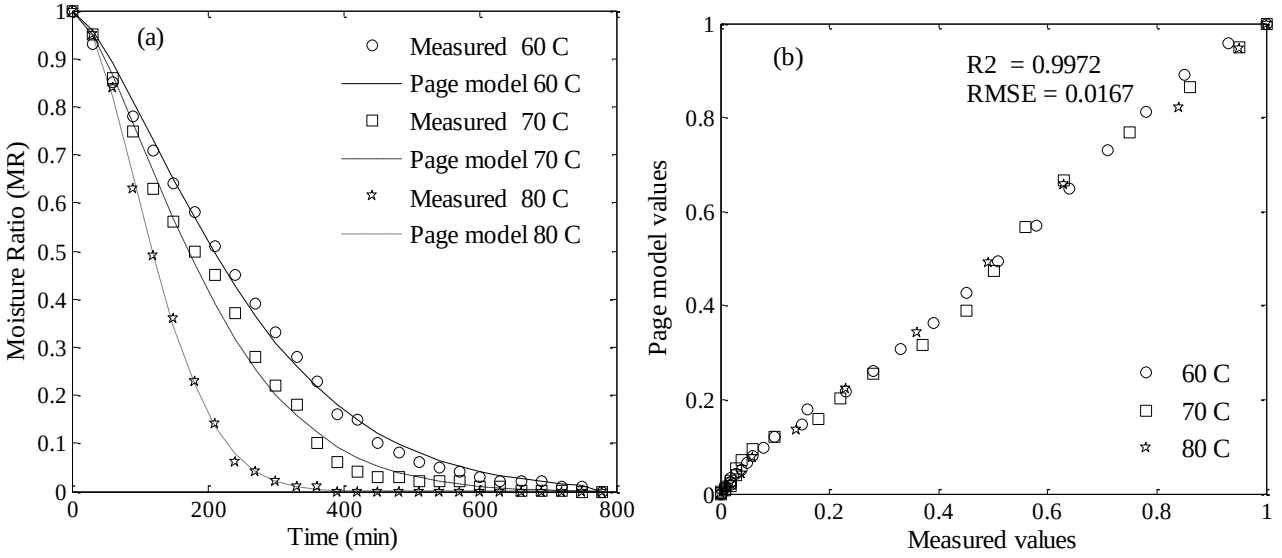

Figure 7 The comparison between the measured and predicted MR values from the Page model, (a) the drying curve (b) the statistical indices

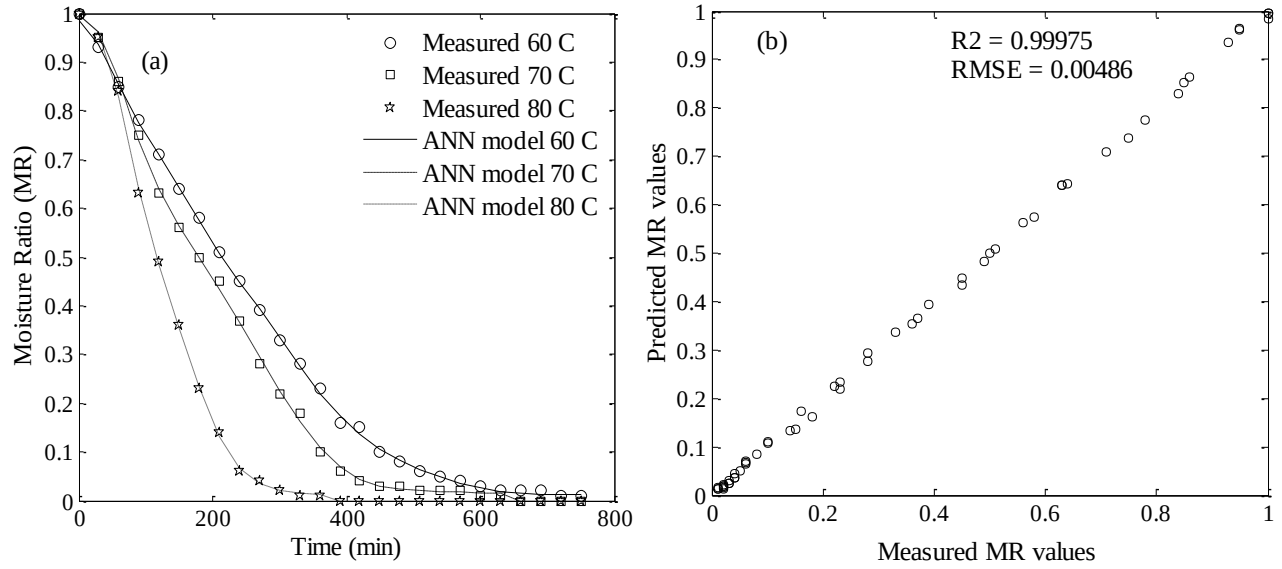

Figure 8 The comparison between of measured and predicted MR value from ANN model (a) the drying curve (b) the statistical indices

had an important effect on the drying kinetics of jackfruit. A higher drying temperature resulted in an increased drying rate and a reduced drying time, moreover, it also reduced specific energy consumption. The page model provided the most optimal representation of the drying behaviour of jackfruit in the FIR dryer. The ANN structure with tan-sigmoid transfer functions, and 12 neurons in hidden layer, was identified as the best model structure. The SEC values at drying temperatures of 60, 70 and 80 °C, were 6.17, 5.77 and 5.38 kWh/kg water respectively. The calculated D_{eff} values ranged from $4.94x10^{-7}$-$10.9x10^{-7}$ m^2/s, and the calculated E_a value was 39.24 kJ/mol.

5. References

[1] Zhang Y, Zhou X, Zhong J, Tan L, Liu C. Effect of pH on emulsification performance of a new functional protein from jackfruit seeds. Food Hydrocoll. 2019;93:325-34.

[2] Doymaz İ. Evaluation of some thin-layer drying models of persimmon slices (*Diospyros kaki* L.). Energ Convers Manag. 2012;56:199-205.

[3] Meziane S. Drying kinetics of olive pomace in a fluidized bed dryer. Energ Convers Manag. 2011;52(3):1644-9.

[4] Shi Q, Zheng Y, Zhao Y. Mathematical modeling on thin-layer heat pump drying of yacon (*Smallanthus sonchifolius*) slices. Energ Convers Manag. 2013;71:208-16.

[5] Song X, Hu H, Zhang B. Drying characteristics of Chinese Yam (*Dioscorea opposita Thunb*.) by far-infrared radiation and heat pump. J Saudi Soc Agric Sci. 2018;17(3):290-6.

[6] Riadh MH, Ahmad SAB, Marhaban MH, Soh AC. Infrared Heating in Food Drying: An Overview. Dry Tech. 2015;33(3):322-35.

[7] Ruiz Celma A, Rojas S, Lopez-Rodríguez F. Mathematical modelling of thin-layer infrared drying of wet olive husk. Chem Eng Process. 2008;47(9):1810-8.

[8] Thanimkarn S, Cheevitsopon E, Jongyingcharoen JS. Effects of vibration, vacuum, and material thickness on infrared drying of *Cissus quadrangularis* Linn. Heliyon. 2019;5(6):1-7.

[9] Ning X, Lee J, Han C. Drying characteristics and quality of red ginseng using far-infrared rays. J Ginseng Res. 2015;39(4):371-5.

[10] Miraei Ashtiani S-H, Salarikia A, Golzarian MR. Analyzing drying characteristics and modeling of thin

layers of peppermint leaves under hot-air and infrared treatments. Inform Process Agric. 2017;4(2):128-39.
[11] Movagharnejad K, Nikzad M. Modeling of tomato drying using artificial neural network. Comput Electron Agric. 2007;59(1):78-85.
[12] Erbay Z, Icier F. A review of thin layer drying of foods: theory, modeling, and experimental results. Crit Rev Food Sci Nutr. 2010;50(5):441-64.
[13] Kantrong H, Tansakul A, Mittal GS. Drying characteristics and quality of shiitake mushroom undergoing microwave-vacuum drying and microwave-vacuum combined with infrared drying. J Food Sci Tech. 2014;51(12):3594-608.
[14] Lertworasirikul S. Drying kinetics of semi-finished cassava crackers: a comparative study. LWT - Food Sci Tech. 2008;41(8):1360-71.
[15] Onwude D, Hashim N, Nawi N, Abdan K. Modelling the convective drying process of pumpkin (*Cucurbita moschata*) using an artificial neural network. Int Food Res J. 2016;23:237-43.
[16] Jena S, Sahoo A. ANN modeling for diffusivity of mushroom and vegetables using a fluidized bed dryer. Particuology. 2013;11(5):607-13.
[17] Nazghelichi T, Kianmehr MH, Aghbashlo M. Prediction of carrot cubes drying kinetics during fluidized bed drying by artificial neural network. J Food Sci Tech. 2011;48(5):542-50.
[18] Behroozi Khazaei N, Tavakoli T, Ghassemian H, Khoshtaghaza MH, Banakar A. Applied machine vision and artificial neural network for modeling and controlling of the grape drying process. Comput Electron Agric. 2013;98:205-13.
[19] Menlik T, Özdemir MB, Kirmaci V. Determination of freeze-drying behaviors of apples by artificial neural network. Expert Syst Appl. 2010;37(12):7669-77.
[20] Kaveh M, Rasooli Sharabiani V, Amiri Chayjan R, Taghinezhad E, Abbaspour-Gilandeh Y, Golpour I. ANFIS and ANNs model for prediction of moisture diffusivity and specific energy consumption potato, garlic and cantaloupe drying under convective hot air dryer. Inform Process Agric. 2018;5(3):372-87.
[21] Sahdev RK, Kumar M, Dhingra AK. Development of empirical expression for thin layer groundnut drying under open sun and forced convection modes. Agric Eng Int. 2017;19(4):152-8.
[22] Artnaseaw A, Theerakulpisut S, Benjapiyaporn C. Drying characteristics of Shiitake mushroom and Jinda chili during vacuum heat pump drying. Food Bioprod Process. 2010;88(2):105-14.
[23] Saeed IE, Sopian K, Zainol Abidin Z. Drying characteristics of roselle: study of the two-term exponential model and drying parameters. Agric Eng Int. 2008;10:1-27.
[24] Triratanasirichai K, Dongbang W, Pirompugd W. Mathematical modeling of drying characteristics of chilies in a rotating fluidized bed technique. Am J Appl Sci. 2011;8:979-83.
[25] Madhiyanon T, Phila A, Soponronnarit S. Models of fluidized bed drying for thin-layer chopped coconut. Appl Therm Eng. 2009;29(14):2849-54.
[26] Omolola AO, Kapila PF, Silungwe HM. Mathematical modeling of drying characteristics of Jew's mallow (*Corchorus olitorius*) leaves. Inform Process Agric. 2019;6(1):109-15.
[27] Nadian MH, Rafiee S, Aghbashlo M, Hosseinpour S, Mohtasebi SS. Continuous real-time monitoring and neural network modeling of apple slices color changes during hot air drying. Food Bioprod Process. 2015: 94:263-74.
[28] Menges HO, Ertekin C. Thin layer drying model for treated and untreated Stanley plums. Energ Convers Manag. 2006;47(15):2337-48.
[29] Aghbashlo M, Kianmehr MH, Arabhosseini A. Modeling of thin-layer drying of potato slices in length of continuous band dryer. Energ Convers Manag. 2009;50(5):1348-55.
[30] Guiné RPF, Pinho S, Barroca MJ. Study of the convective drying of pumpkin (*Cucurbita maxima*). Food Bioprod Process. 2011;89(4):422-8.
[31] Pardeshi IL, Arora S, Borker PA. Thin-Layer drying of green peas and selection of a suitable thin-layer drying model. Dry Tech. 2009;27(2):288-95.
[32] Hernández-Péreza JA, García-Alvaradob MA, Trystrama G, Heyd B. Neural networks for the heat and mass transfer prediction during drying of cassava and mango. Innovat Food Sci Emerg Tech. 2004:5:57-64.